A Multi-path Model for Disturbance Propagation in Electrical Power Networks

Akash Kumar Mandal, *Graduate Student Member, IEEE,* Arpan Malkhandi, *Graduate Student Member, IEEE,* Swades De, *Senior Member, IEEE,* Nilanjan Senroy, *Senior Member, IEEE,* Sukumar Mishra, *Senior Member, IEEE*

***Abstract*—This paper deals with the nature of propagation of disturbance spectrum through the power lines of an electric power system. A multi-path propagation model is proposed based on the reflection and refraction theory of wave propagation. The developed model captures the spatio-temporal aspect of disturbance propagation and is validated for a wide band of frequency. The proof of concept for the developed model is shown on a 2-bus system with a disturbance at a point between the buses. Results are validated in time domain with electromagnetic transient simulation programming.**

***Index Terms*—Multi-path wave propagation, disturbance propagation, harmonic stability, continuous wavelet transform, electromagnetic transient simulation programming**

I. Introduction

DISTURBANCES in traditional power system networks are caused by external events like lightning strike or corona discharges. These perturbations causes distortion of sinusoidal voltage and current waveform, which travel throughout the transmission system and eventually dies out. However, the proliferation of power electronic switching based loads and sources has resulted in injection of periodic disturbances from the power system elements. It is noted that the power electronics interfaced systems employ closed loop controllers driven by sensed voltage and current at the point of grid connection. From their stability perspective, it is necessary to study the propagation of disturbances arising at a particular point in the network. This work focuses on the development of a mathematical model of disturbance propagation for both transmission and distribution networks.

A. State of the Art and Motivation

The study of the effect of disturbance on the network components includes two aspects: the nature of perturbation and the topology of the network. Any disturbance is characterized through its harmonic content. Real world disturbances like faults, load changes, or lightning strikes on power lines are analytically broken down into Fourier series and specific frequencies of interest may be chosen to evaluate their effect on the overall system stability. The harmonics of interest depends on the power system components under study. Power system designers have traditionally focused on the propagation of electro-mechanical disturbances caused by conventional synchronous generators [1], [2], [3], [4]. Disturbances in the high frequency band were negligible due to the presence of rotating machine inertia in the power system. However, the rapid proliferation of grid tied converters and switching loads has resulted in switched power generation and their fast-acting control systems, leading in the shift of stability analysis from a narrow low frequency band to a wider band ranging up to a few kilo hertz, i.e., the super-synchronous and high frequency band [5], [6]. Power electronics based energy conversion has resulted in injection of several harmonic disturbances in both AC and DC power systems. In microgrids with only converter based energy sources sustained inter-harmonic injections requires the analysis of disturbance propagation in the low voltage distribution systems as well. This necessitates the development of a proper wide band disturbance propagation model and therefore forms an integral part of any disturbance propagation study.

Disturbance propagation is spatio-temporal in nature, i.e., both the information of its magnitude at all buses in a network, and its behavior in time is of importance. In this respect, the type of modeling of the power lines and its harmonic propagation quality plays an important role in the accuracy to real time disturbance features. A HARMFLO (Harmonic Load flow) algorithm was proposed utilizing the complex power flow equations and line impedance as reflection-less lumped parameters [7], [8]. Newton-Raphson method was used to solve the set of nonlinear algebraic equations. This method captures the steady state features of a sustained disturbance but may not be useful in tracking a transient perturbation in the system. In order to model and validate the propagation of electro-mechanical oscillations, the swing equation has been used considering a lumped assumption of line impedance [9], [10], [11], [12]. In either of the previous developments, it is difficult to gather the spatio-temporal information from the involved differentials. Also, a grouped analysis looses the alternate dimension's information when a multi-modal transformation is applied thereafter to extract frequency data from the obtained wave function. Furthermore, wave refraction and reflection property has not been considered, limiting the delay information about a frequency component. Such a consideration of lumped impedance information in these models fails in accommodating the variability of the disturbance impact between a distribution system and a transmission system. Recent literature [11], [13] takes a data based approach to disturbance propagation analysis, but does not analyze its

This work was supported by the Science and Engineering Board, DST, under Grant CRG/2019/002293, and the INAE under the Abdul Kalam Technology Innovation National Fellowship.

The authors are with the Department of Electrical Engineering and Bharti School of Telecommunication, Indian Institute of Technology Delhi, New Delhi 110016, India.

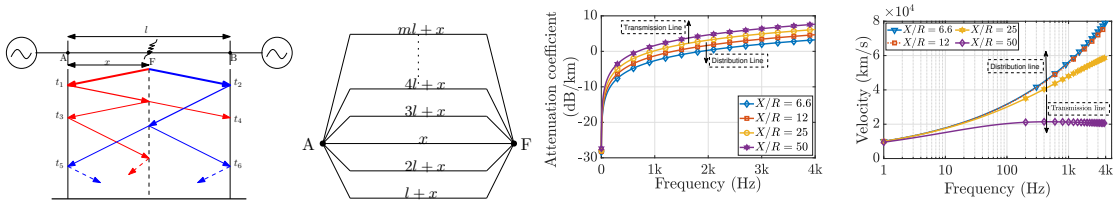

Fig. 1: (a) Lattice diagram with disturbance at node F in line $A-B$; (b) equivalent multi-path model for disturbance propagation in electrical grids observed at node A for m multi-paths.

wide band manifestation. Since, such an approach is based on data collection and analysis phases, the time complexity of such methods precludes the possibility of real-time disturbance analysis profile on the order of the impact that a disturbance wave renders. Furthermore, this kind of data-driven analysis is insufficient for pre-event risk analysis of a power system subjected to different disturbance profiles. However, further research could prove valuable in maturing this approach of power system disturbance propagation modeling.

B. Contribution and Significance

In this paper, a multi-path propagation model based approach for analyzing power system disturbance propagation for a wide band frequency spectrum is proposed. The major contributions of this work are as follows:

1) A multi-path model based on Bewley's lattice diagram [14], [15] is proposed to capture the spatio-temporal propagation of disturbance, aiding power system planning.
2) An algorithm is proposed for parameter estimation of the multi-path model, followed by its application in disturbance profile analysis at a node. The correctness of the proposed multi-path model is verified using electromagnetic transient simulation programming (EMTP).
3) The proposed multi-path modeling approach captures a wide band disturbance study, thereby aiding the stability analysis in grids with higher renewable penetration, which is done for a wide band of frequency spectra. This further reduces the need to solve nonlinear differential equations for disturbance profile analysis at a graph node.
4) The consideration of distributed parameters in this analysis helps in differentiating the impact of any disturbance for different power system ratings, which can be achieved by varying the X/R ratio of the power lines.
5) The proposed modeling approach keeps both the time and frequency information coexistent, which helps in identifying the system performance under disturbance at different times based on the dominant frequency components in the disturbance wave. This makes the modeling invariant to the disturbance profile that the grid might suffer.

The work in this paper captures the spatio-temporal impact of disturbance in a network at a generic point, while keeping the frequency information intact. The applicability of this model is not limited to the use-case discussed here; it can be extended to model wave propagation profile through any media.

The layout of the paper is as follows: The proposed multi-path model is presented in Section II, followed by multi-path model parameter analysis in Section III, and model validation in Section IV. Section V concludes the paper.

II. Modeling

A. System Model

Let a disturbance wave be initiated at point F as shown in Fig. 1(a), which travels to both ends of the line $A-F-B$. This wave suffers multiple reflections and refractions at each node it encounters in its path leading to different frequency components of the disturbance wave, each showing different propagating characteristics [16], [17]. This phenomenon can be equivalently thought of as a wave propagating between a source and a receiver through multiple paths generated as a result of multiple nodal reflections and refractions, which gets attenuated/amplified/phase shifted as a function of characteristic impedance of the power line. The proposed multi-path model corresponding to Fig. 1(a) is shown in Fig. 1(b).

The disturbance encounters multiple spatio-temporal reflections and refractions as shown in Fig. 1(a) using t_i, $i \in \{1, \cdots, 6, \cdots\}$. Therefore, the path length traversed by each such reflected/refracted component changes as $l+x$ in the first reflection instance at node B, $2l+x$ in second such instance, and $ml+x$ in the m^{th} such instant. This is congruous to visualizing the disturbance wave traveling through m multi-paths of varying lengths as shown in Fig. 1(b), thus developing the idea of multi-path wave propagation in power lines. The next subsection proposes a mathematical model to capture disturbance propagation using this idea.

B. Multi-path Model of Disturbance Propagation

Following the system model defined in Fig. 1, it can be seen that the disturbance arising at a point F on the powerline defined between A and B will suffer multiple reflection and refraction at each of these nodes and lay an effective disturbance profile at the observation node. If the observation is taken at node A, then possible paths that the disturbance wave would traverse are $F \rightarrow A$ (line-of-sight path), $F \rightarrow A \rightarrow F \rightarrow A$, $F \rightarrow B \rightarrow F \rightarrow A$, $F \rightarrow A \rightarrow F \rightarrow B \rightarrow F \rightarrow A$, $F \rightarrow B \rightarrow F \rightarrow B \rightarrow F \rightarrow A$, $F \rightarrow B \rightarrow F \rightarrow A \rightarrow F \rightarrow A$, and so on. Thus, a single powerline segment carrying disturbance can be thought of as multiple disturbance relaying paths between the disturbance point and the observation node, as shown in Fig. 1(b). The mathematical formulation of the proposed multi-path model [18] is expressed as

$$i_{A,F}(t) = \sum_{f \in \mathscr{F}} \theta(f,t) e^{j\delta(f,t)} \sum_{m=1}^{L(f,t)} g_m(f) e^{-j\phi_{g_m}(f)} \times A_m(f) e^{-j2\pi f \tau_{d,m}(f)} \quad (1)$$

TABLE I: Disturbance signatures (current, in A) for a 123 kV grid.

Freq. (Hz)	$\mathbf{t = 0}$ s	$\mathbf{t = 5}$ ms	$\mathbf{t = 50}$ ms
500	$7.6e^{j108.31}$	$5.7e^{j97.22}$	$7.6e^{j106.63}$
1000	$25.4e^{j120.07}$	$20.9e^{-j54.62}$	$5.4e^{j119.17}$
2000	$72.3e^{j139.39}$	$78.9e^{-j129.12}$	$90.3e^{j138.95}$
4000	$25e^{j178.79}$	$24.7e^{-j135.36}$	$23e^{j178.58}$

where $i_{A,F}(t)$ is the impact of the disturbance generated at node F at some other node A observed at time instant t, $\theta(f,t)$ is the amplitude of the f^{th} frequency component generated using modal decomposition of the disturbance current given by $i_F(t)$ observed in the time window T, and $\delta(f,t)$ is its phase at time t. $\mathscr{F}$ is the frequency array defined by the modal decomposition of $i_F(t)$, $h_m(f) = g_m(f)e^{-j\phi_{g_m}(f)}$ is the complex gain offered by different multi-paths to different frequency components of the disturbance wave traveling through it, thus capturing the wide-band effect profile of disturbance wave. $L(f,t) = L$ is the total number of significant multi-paths that capture at least ϵ energy fraction of the total disturbance wave, and for the sake of easy analysis can be considered independent of f and t in the scope of this work. With time the energy in a disturbance wave would dissipate due to spatio-temporal attenuation offered by the propagating medium and thus L should decrease as time progresses. Furthermore, the consideration of effective number of multi-paths for a frequency component contributing relatively lesser fraction in the total wave energy, will be lesser owing to less energy content in that particular frequency component of the wave. $A_m(f)$ is the frequency dependant amplitude attenuation with the distance traversed by the disturbance, and the phase change due to the delay is captured using $e^{-j2\pi f\tau_{d,m}(f)}$.

The complex propagation constant for a cable is a function of its primary parameters R', G', C', and L' denoting respectively the per unit resistance, conductance, capacitance, and inductance of the power line, and is given as [18]

$$\gamma(\omega) = \sqrt{(R' + j\omega L')(G' + j\omega C')} = \alpha(\omega) + j\beta(\omega). \quad (2)$$

The real part in (2) given by $\alpha(f)$ governs the frequency dependent attenuation, and the imaginary part governs the phase velocity given by $v_p = \frac{\omega}{\beta(f)}$, with $\omega = 2\pi f$. From the expression in (2), it can be concluded that at higher side of the frequency spectra $\beta(f) = \kappa f$ with κ being a frequency-independent constant of proportionality, therefore the phase velocity $v_p = \frac{2\pi}{\kappa}$. However, at lower side of spectra $v_p = \frac{2\pi f}{\beta(f)}$. Thus, higher frequency components travel at same speed while lower frequency components do not, in a power system model with high $\frac{X}{R}$. Therefore, the amplitude attenuation is given by $A_w(f) = e^{-\alpha(f)(ml+x)}$. Following the analysis of γ, delay can be characterized as $\tau_{d,m}(f) = \frac{(ml+x)\beta(f)}{\omega}$. Substituting these in (1), we have

$$i_{A,F}(t) = \sum_f \theta(f,t)e^{j\delta(f,t)} \sum_{m=1}^{L(f,t)} g_m(f)e^{-j\phi_{g_m}(f)} \times e^{-\{\alpha(f)+j\beta(f)\}(ml+x)} \quad (3)$$

where x is the distance of the disturbance point from the observation node, and l is the length of the line defined between nodes A and B in Fig. 1(a). Also, $g_m(f)$ defines the fraction of energy traveling through path m for the component with frequency f, therefore $\sum_f g_m(f) < \varepsilon_m$, and $\sum_{m=1}^{L(f,t)} g_m(f) = 1$, where ε_m is the fraction of the disturbance wave's energy along the path m. Since, the energy of the wave function is captured in the model, the circuit theoretic validation satisfies by default. Therefore, $L(f,t) := \{L | \sum_{m=1}^{L} \varepsilon_m \geq \epsilon\}$ allows control over the precision of the model at the cost of computational complexity.

Remark 1. *The parameters of interest are $L(f,t)$ denoting the number of significant multi-paths for the frequency component f at time t, and the frequency dependant complex gain $g_m(f)e^{-j\phi_{g_m}(f)}$ parameterized by $[g_m(f), \phi_{g_m}(f)]$, offered by each of the multi-paths to different frequency components. The next section provides estimation of these parameters.*

III. Parametric Analysis of the Multi-path Model

A. Parameter Estimation

For the parameters stated in Remark 1, an Algorithm 1 is proposed for the optimal estimation of the hyper-parameters used in (3). Primarily, the disturbance waveform at node F and its impact at node A are captured in two time arrays d_{i_F} and $d_{i_{A,F}}$, respectively. Subsequently, d_{i_F} is decomposed into its major frequency components and their respective phases using continuous wavelet transform (CWT) [19] as the modal decomposition technique to preserve both time and frequency information within a certain bound of uncertainties. CWT

Algorithm 1: Disturbance profile analysis at node A due to a disturbance at node F

```
Result: Disturbance profile at an observation node
Initialize a disturbance i_F of duration Δ
d_{i_F} → time array of dist. samples for duration Δ
d_{i_A} → time array of disturbance profile at node A
CWT coefficients (:= θ(k,t)) → |CWT(d_{i_F})|
Frequency array (:= 𝓕) → CWT(d_{i_F})
Find α(f) and β(f) using (2)
Residual energy threshold := υ_th
Set residual energy (:= υ) > υ_th
Set tolerance (:= tol)
while ||υ − υ_th|| > tol do
    Multi-path count (:= mpc) = 1
    for m = 1 : mpc do
        for f ∈ do
            Search: g_m(f) ∈ (0, 1] and
              φ_{g_m(f)} ∈ [−π, π]
            Evaluate i_{A,F}(t)
        end
        d_{i_{A,F}} → time series estimated data at node A
          using (3).
    end
    Update υ = ||E_{d_{i_{A,F}}} − E_{d_{i_A}}||
    mpc → mpc + 1
end
```

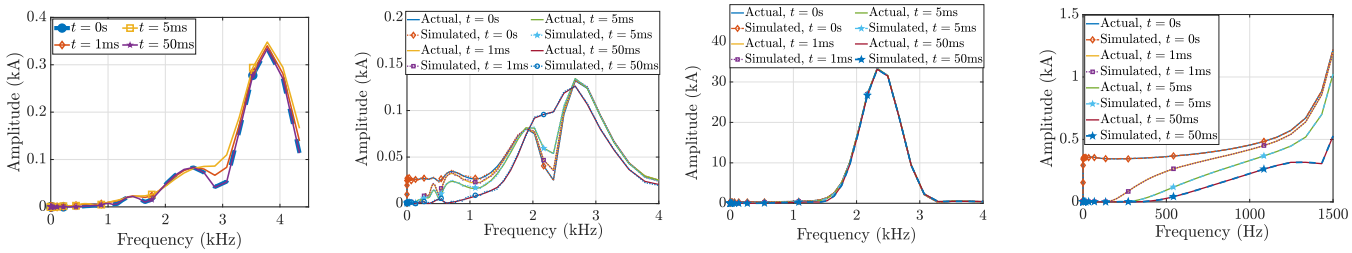

(a) (b) (c) (d)

Fig. 2: Disturbance profile at (a) disturbance node, (b) observation node (123 kV), (c) observation node (33 kV), (d) zoomed view Fig. 3(c).

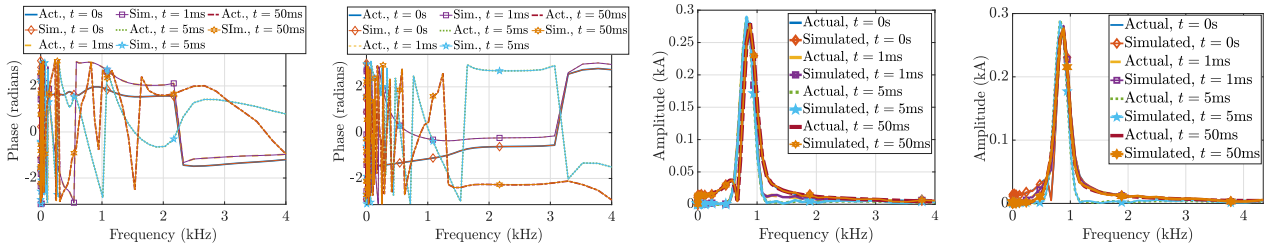

(a) (b) (c) (d)

Fig. 3: Disturbance phase (a) 123 kV, (b) 33 kV; Disturbance profile on line 7-8 for IEEE 9-bus system (c) normal, (d) line-to-ground short.

with the Morse wavelet, symmetry parameter 3, and time-bandwidth product of 60 is used, owing to zero demodulate skewness, minimal time-domain sidelobes and frequency-domain asymmetry corresponding to it. The attenuation parameters $\alpha(f)$ and $\beta(f)$ are calculated using (2). An energy threshold and tolerance given by υ_{th} and tol respectively is defined to find the reinforced values of complex multi-path gains and therefore define the number of significant multi-paths to consider. $g_m(f)$ and $\phi_{g_m}(f)$ are found using a reinforced grid search defined on $(0, 1]$ and $[-\pi, \pi]$. This process is repeated with increasing the multi-path count until the residual energy was found within a predefined bound of υ_{th}. This approach was found to give a sufficiently accurate result as can be seen from the matching simulated disturbance profile in Fig. 2(b) and (c) rendered by the model in (3) for a transmission and distribution system respectively. In this analysis, $\upsilon_{th} = 0.99$ and $tol = 10^{-5}$ was used. E_{x_t} is defined as the energy of time series data x_t in Algorithm 1, and is given as $E_{x_t} = x_t \odot \Delta_t {x_t}^T$, with Δ_t being the time instance series corresponding to the time series data x_t. The model was found to perform in accordance to PSCAD results with ≤ 4 multi-path count for all frequencies in $\mathscr{F}$.

B. Model Parameter Analysis

Using the parameters estimated through Algorithm 1, the attenuation and delay profiles for disturbance is generated (Fig. 1). From Fig. 1(d) it is observed that for $X/R = 50$, corresponding a high voltage transmission line, high frequency components travel with the same velocity, which validates our proposition in Subsection II-B. It can further be noted from Fig. 1(c) that this behaviour changes as the X/R ratio drops and becomes typical of a low voltage transmission or distribution system. In such cases, the velocity of the frequency components rises non-linearly with the corresponding frequency component of the disturbance wave. This gives further insight into the necessity of developing a wide-band analysis as presented in this work. These graphs provide an insight into the intensity with which a disturbance can impact a part of the power system. Furthermore, as this approach allows an a-priori modeling of a disturbance-ridden power system, for a particular injection-observation node pair, the proposed approach achieves the characterization of disturbance propagation in power lines as a planning problem.

IV. Multi-path Model Validation

A step load change of 30 MW for a duration of 0.05 s was simulated, thus generating a wideband frequency disturbance on a 2-bus system rated at 123 kV and 33 kV in EMTP (PSCAD) to validate the mathematical model proposed in (3). Current measurements at disturbance and observation node were sampled at 10 MHz. Fig. 2(a) shows the disturbance profile given to the system. Here, a few observations are noted, to understand the necessity and strength of the proposed formulation. From the frequency domain plot in Fig. 2(a) for different time stamps, it can be seen that the contribution of a particular frequency component in the disturbance waveform is time-dependant, indicating that not all frequency components are available at all times. This corroborates the proposition of different phase velocities for different frequency components. Furthermore, the higher side of the spectra in Fig. 2(b) and Fig. 2(c) can be seen validating the premise of equi-speed propagation for these components.

Figs. 2(b) and 2(c) show the comparison between the actual disturbance profile at node A captured using PSCAD and the disturbance profile as predicted by the multi-path model defined in (3) for the transmission and distribution system respectively. It can be seen that these waveforms overlap very well with a maximum root mean square error of 4.37×10^{-5} and 1.1×10^{-5} for Fig. 2(b) and (c) corresponding to all

time instances. A similar match can be observed for their corresponding phase patterns too from Figs. 3(a) and 3(b) for 123 kV and 33 kV grids, respectively. These graphs also corroborate the theory of different frequency components reaching the observation node through different multi-paths as can be seen through the crossovers between the graphs depicting different temporal snapshots. For instance, the component corresponding to 2 kHz can be seen to gain weight in the spectra at 50 ms as opposed to its value at times of lesser order, which is a result of it traveling through various multi-paths and thus rendering delayed contributions at the observation node, which would be monotonically declining otherwise. An equivalent inference based on data can be drawn from Table I corresponding to 123 kV grid.

From Fig. 2(c), for a 33 kV line, we can see that almost all frequency components are present at all time instants at different magnitudes with different temporal attenuations. Such frequency dependence of disturbance wave propagation can only be addressed through a modeling as proposed here. The zoomed-in region of Fig. 2(c) shown in Fig. 2(d) helps to verify the same for frequency band of 0-1500 Hz. It can be thus seen that the impact of disturbance on power system health becomes more detrimental as the rated line voltage drops, by letting the disturbance survive for a longer time window. Further, a step load change of 10 MW/ 132 kV for a duration of 0.05 second was applied on bus 6 of an IEEE 9-bus system. Thus, the extension of the proposed model was validated for an observation point on line 7-8 in normal condition as well as for line-to-ground short circuit in line 4-5, as shown in Figs. 3(c) and 3(d), respectively. The actual and simulated graphs show a good overlap with nRMSE below 6.47×10^{-5} and 2.37×10^{-5} in the respective cases. This validates the applicability of the proposed multi-path model in bigger power grid systems.

V. Conclusion

This work has established a multi-path model based approach to disturbance propagation analysis in a two terminal power system segment using the concept of wave reflection and refraction theory as it encounters a grid node. The EMTP simulation shows that this model was able to capture disturbance for both transmission and distribution lines at an observation node with strong accuracy. It was further observed that the idea of multi-path disturbance propagation can explain better the delay and phase offsets that a single frequency component shows. The proposed model offers a possibility to carry out investigations for different network topologies for any kind of disturbance it may encounter. Further, as demonstrated through simulation results, the model can be extended to capture disturbance propagation profile in bigger power grid systems, with non-linearities induced by grid-tied inverters, switching loads, and under system abnormalities, such as faults. Therefore, this approach of wide band disturbance study gains over the existing disturbance propagation study [20] through a detailed information of delay, phase, and intensity content for a frequency component of a disturbance wave, as a system planning exercise. Hence, this model can be used to characterize a power grid into a system of closed form equations, thereby aiding the determination of fault locations and ripple propagation analysis set by it.

References

[1] M. Parashar, J. S. Thorp, and C. E. Seyler, "Continuum modeling of electromechanical dynamics in large-scale power systems," *IEEE Trans. Circuits Syst. I: Regular Papers*, vol. 51, no. 9, pp. 1848–1858, 2004.

[2] T. Bi, J. Qin, Y. Yan, H. Liu, and K. E. Martin, "An approach for estimating disturbance arrival time based on structural frame model," *IEEE Trans. Power Syst.*, vol. 32, no. 3, pp. 1741–1750, 2016.

[3] D. Huang, J. Qin, H. Liu, J. H. Chow, J. Zhao, T. Bi, L. Mili, and Q. Yang, "An analytical method for disturbance propagation investigation based on the electromechanical wave approach," *IEEE Trans. Power Syst.*, vol. 36, no. 2, pp. 991–1001, 2021.

[4] S. Tamrakar, M. Conrath, and S. Kettemann, "Propagation of disturbances in AC electricity grids," *Scientific reports*, vol. 8, no. 1, pp. 1–11, 2018.

[5] A. Malkhandi, N. Senroy, and S. Mishra, "On the parametric dependence of the stability of a current controlled grid tied inverter," in *Proc. 20th International Conf. on Intelligent System Application to Power Systems (ISAP)*. IEEE, 2019, pp. 1–5.

[6] A. Malkhandi, N. Senroy, and S. Mishra, "Return ratio shaping approach to stabilize inverter-weak grid system," *IEEE Trans. Energy Conver.*, vol. 36, no. 1, pp. 253–263, 2020.

[7] G. T. Heydt and W. Grady, "The HARMFLO code: Version 4. 0: User's guide," Purdue Univ., Lafayette, IN (USA). Dept. of Electrical Engineering; Electric, Tech. Rep., 1986.

[8] S. Herraiz, L. Sainz, and J. Clua, "Review of harmonic load flow formulations," *IEEE Trans. Power Deliv.*, vol. 18, no. 3, pp. 1079–1087, 2003.

[9] J. S. Thorp, C. E. Seyler, and A. G. Phadke, "Electromechanical wave propagation in large electric power systems," *IEEE Trans. Circuits Syst. I: Fundamental Theory and Applications*, vol. 45, no. 6, pp. 614–622, 1998.

[10] D. Huang, H. Liu, J. Zhao, T. Bi, and Q. Yang, "A novel non-uniform frame structure model for power system disturbance propagation analysis," *IEEE Trans. Power Syst.*, pp. 1–1, 2021.

[11] N. Ma and D. Wang, "Extracting spatial-temporal characteristics of frequency dynamic in large-scale power grids," *IEEE Trans. Power Syst.*, vol. 34, no. 4, pp. 2654–2662, 2019.

[12] L. A. Torres-Sánchez, G. T. Freitas de Abreu, and S. Kettemann, "Analysis of the dynamics and topology dependencies of small perturbations in electric transmission grids," *Phys. Rev. E*, vol. 101, p. 012313, Jan 2020.

[13] H. Ul Banna, S. K. Solanki, and J. Solanki, "Data-driven disturbance source identification for power system oscillations using credibility search ensemble learning," *IET Smart Grid*, vol. 2, no. 2, pp. 293–300, 2019.

[14] C.-K. Lee and Y.-J. Shin, "Detection and assessment of i amp;c cable faults using time–frequency r-cnn-based reflectometry," *IEEE Trans. Ind. Electron.*, vol. 68, no. 2, pp. 1581–1590, 2021.

[15] T. Lan, Y. Li, and X. Duan, "High fault-resistance tolerable traveling wave protection for multi-terminal vsc-hvdc," *IEEE Trans. Power Deliv.*, vol. 36, no. 2, pp. 943–956, 2021.

[16] O. Naidu and A. K. Pradhan, "A traveling wave-based fault location method using unsynchronized current measurements," *IEEE Trans. Power Deliv.*, vol. 34, no. 2, pp. 505–513, 2019.

[17] S. Roy, W. Ju, N. Nayak, and B. Lesieutre, "Localizing power-grid forced oscillations based on harmonic analysis of synchrophasor data," in *Proc. 55th Annu. Conf. Inf. Sci. Syst. (CISS)*. IEEE, 2021, pp. 1–5.

[18] M. Zimmermann and K. Dostert, "A multipath model for the powerline channel," *IEEE Trans. commun.*, vol. 50, no. 4, pp. 553–559, 2002.

[19] R. S. Pathak, *The wavelet transform*. Springer Science & Business Media, 2009, vol. 4.

[20] A. Greenwood, "Electrical transients in power systems,," New York, NY (USA); John Wiley and Sons Inc., 1991.